

## Article

# Quantitative Assessment of Periodontal Bacteria Using a Cell-Based Immunoassay with Functionalized Quartz Crystal Microbalance

Satit Rodphukdeekul <sup>1,2</sup>, Miyuki Tabata <sup>2</sup> , Chindanai Ratanaporncharoen <sup>2</sup>, Yasuo Takeuchi <sup>3</sup> , Pakpum Somboon <sup>1</sup>, Watcharee Boonlue <sup>4,5</sup>, Yuji Miyahara <sup>2,\*</sup> and Mana Sriyudthsak <sup>6,\*</sup>

- <sup>1</sup> Biomedical Engineering Program, Faculty of Engineering, Chulalongkorn University, Bangkok 10330, Thailand; satit.rod@student.chula.ac.th (S.R.); pakpum.s@chula.ac.th (P.S.)
  - <sup>2</sup> Institute of Biomaterials and Bioengineering, Tokyo Medical and Dental University, Tokyo 101-0062, Japan; tabata.bsr@tmd.ac.jp (M.T.); r.chindanai@gmail.com (C.R.)
  - <sup>3</sup> Department of Periodontology, Faculty of Dentistry, Tokyo Medical and Dental University, Tokyo 113-8510, Japan; takeuchi.peri@tmd.ac.jp
  - <sup>4</sup> Department of Nutrition and Dietetics, Faculty of Allied Health Sciences, Chulalongkorn University, Bangkok 10330, Thailand; Watcharee.Bo@chula.ac.th
  - <sup>5</sup> Biosensors and Bioanalytical Technology for Cells and Innovative Testing Device Research Unit, Chulalongkorn University, Bangkok 10330, Thailand
  - <sup>6</sup> Department of Electrical Engineering, Faculty of Engineering, Chulalongkorn University, Bangkok 10330, Thailand
- \* Correspondence: miyahara.bsr@tmd.ac.jp (Y.M.); mana.S@chula.ac.th (M.S.)



**Citation:** Rodphukdeekul, S.; Tabata, M.; Ratanaporncharoen, C.; Takeuchi, Y.; Somboon, P.; Boonlue, W.; Miyahara, Y.; Sriyudthsak, M. Quantitative Assessment of Periodontal Bacteria Using a Cell-Based Immunoassay with Functionalized Quartz Crystal Microbalance. *Chemosensors* **2021**, *9*, 159. <https://doi.org/10.3390/chemosensors9070159>

Academic Editor: Raffaele Velotta

Received: 15 April 2021

Accepted: 22 June 2021

Published: 25 June 2021

**Publisher's Note:** MDPI stays neutral with regard to jurisdictional claims in published maps and institutional affiliations.

**Abstract:** Periodontal disease is an inflammatory disorder that is triggered by bacterial plaque and causes the destruction of the tooth-supporting tissues leading to tooth loss. Several bacteria species, including *Porphyromonas gingivalis* and *Aggregatibacter actinomycetemcomitans*, are considered to be associated with severe periodontal conditions. In this study, we demonstrated a quartz crystal microbalance (QCM) immunoassay for quantitative assessment of the periodontal bacteria, *A. actinomycetemcomitans*. An immunosensor was constructed using a self-assembled monolayer of 11-mercaptopundecanoic acid (11-MUA) on the gold surface of a QCM chip. The 11-MUA layer was evaluated using a cyclic voltammetry technique to determine its mass and packing density. Next, a monoclonal antibody was covalently linked to 11-MUA using 1-ethyl-3-(3-dimethylaminopropyl) carbodiimide/N-hydroxysuccinimide to act as the biorecognition element. The specificity of the monoclonal antibody was confirmed by an enzyme-linked immunosorbent assay. A calibration curve, for the relationship between the frequency shifts and number of bacteria, was used to calculate the number of *A. actinomycetemcomitans* bacteria in a test sample. Based on a regression equation, the lower detection limit was 800 cells, with a dynamic range up to  $2.32 \times 10^6$  cells. Thus, the QCM biosensor in this study provides a sensitive and label-free method for quantitative analysis of periodontal bacteria. The method can be used in various biosensing assays for practical application and routine detection of periodontitis pathogens.

**Keywords:** periodontal bacteria; immunoassays; quartz crystal microbalance biosensors



**Copyright:** © 2021 by the authors. Licensee MDPI, Basel, Switzerland. This article is an open access article distributed under the terms and conditions of the Creative Commons Attribution (CC BY) license (<https://creativecommons.org/licenses/by/4.0/>).

## 1. Introduction

Oral disorders caused by dental caries and periodontal diseases have a profound effect on general health and quality of life. Periodontitis, the sixth most prevalent disease worldwide [1], is a chronic inflammation of periodontal tissue leading to tooth loss. Periodontal diagnosis is conventionally based on clinical and radiographical evaluations that mainly consist of measurements of probing depth, bone level, bleeding and tooth mobility. However, the data obtained from these methods only reflect the results of disease progression and do not necessarily present the current disease activities [2].

Inflammatory periodontal destruction is mainly caused by chronic infection of bacteria. More than 700 bacterial species are reportedly found in the oral cavity [3] and multiple bacterial species form biofilm and reside in periodontal pockets. It is presently recognized that an imbalance of microbiota, called dysbiosis, disrupts host homeostasis and causes periodontal destruction. Previous studies have reported the involvement of specific bacterial species as keystone pathogens that cause dysbiosis [4] and increase the number of some specific bacteria in periodontitis patients.

The main cause of periodontitis is the appearance of a mixed red-complex bacterial infection, including *Porphyromonas gingivalis* (*P. gingivalis*), *Treponema denticola* (*T. denticola*), *Tannerella forsythia* (*T. forsythia*) and other Gram-negative anaerobic species, particularly, *Aggregatibacter actinomycetemcomitans* (*A. actinomycetemcomitans*) and *Prevotella intermedia* (*P. intermedia*), that is colocalized in dental plaque [5–7]. Evidence from previous studies suggests that the concentrations of some bacteria in the oral cavity of the patients are higher than those in healthy people. The existence of a single or multiple species of the red-complex bacteria with a specific threshold may serve as a potential indicator and predictor of periodontitis progression [8–10]. However, it is difficult to diagnose pathogenic bacteria, as the most conventional methods rely on laboratory-based techniques, such as cell culture, microscopic analysis and biochemical assays [11]. Additionally, specific pathogens are difficult to culture in vitro or require a long cultivation period. Nevertheless, extensive efforts have been made to diagnose bacterial infections in an early state to prevent irreversible damage of the patient's tooth.

In 2018, He et al. reported chairside microorganisms test kits, i.e., the Omnigene diagnostics test, Evalusite kit and PerioScan kit [2]. These test kits were developed to detect multiple bacteria, such as *P. gingivalis*, *P. intermedia* and *A. actinomycetemcomitans*, using different principles: a nucleic acid hybridization-based assay, sandwich enzyme immunoassay [12] and a N-benzoyl-DL-arginine-2 naphthylamide (BANA) hydrolysis reaction [13], respectively. However, these clinical tools are not ideal for rapid diagnosis because the Omnigene diagnostics test is time-consuming, the Evalusite kit has low sensitivity and the PerioScan kit is a qualitative test for disease severity [2]. Furthermore, polymerase chain reaction (PCR), the most sensitive technique for clinical specimens, is dependent on target genes, primer sequences and requires DNA extraction procedures [14]. As a result, biosensor technologies have been developed to overcome the limitations. Various types of biosensors, such as electrochemical biosensors based on amperometric, potentiometric, or impedimetric transducers, have been developed for sensitive detection and easy application [15]. However, in the case of bacteria detection, cost-effective and reliable devices are required for practical use, while the fabrication processes of conventional sensors use expensive equipment and facilities.

Over the past two decades, the unique capability of the quartz crystal microbalance (QCM) biosensor-based assays has been particularly attractive in the field of cell biology [16]. QCM is a promising platform with enhanced sensitivity and specificity for the bioanalytical systems, as it was developed as a fast, inexpensive and high sensitivity tool. The aim of this work is to develop a quantitative assessment technique for periodontal bacteria detection using a QCM immunoassay.

## 2. Experimental Methods

### 2.1. Materials

*Aggregatibacter actinomycetemcomitans* (ATCC 43719), *Porphyromonas gingivalis* (ATCC 33277) *Prevotella nigrescens* (ATCC 33563) and *Actinomyces naeslundii* (ATCC 12104) were cultured according to the anaerobic cultural methodology previously described by Uekubo A. et al. [17] and Komazaki R. et al. [18]. Briefly, bacterial cells were cultured in brain–heart infusion (BHI) broth (Oxoid Ltd., Basingstoke, UK) with 5 µg/mL of hemin (Sigma, Poole, UK) at 37 °C for 2 days under anaerobic conditions. All reagents were stored under oxygen-free conditions. For harvesting, the cultured cells were centrifuged at 8000× g for 15 min at 4 °C and the cell pellets were resuspended with phosphate-buffered saline (PBS) and

stored at  $-80\text{ }^{\circ}\text{C}$  until use. The concentration of bacterial samples was determined using a Petroff–Hauser counting chamber under optical microscopy. Anti-*A. actinomycetemcomitans* monoclonal antibody (DSHB Hybridoma Product 325AA2) was purchased from the Developmental Studies Hybridoma Bank, Department of Biology, University of Iowa, USA. The following materials were obtained as indicated: 11-mercaptoundecanoic acid (11-MUA), 1-ethyl-3-[3-dimethylaminopropyl]carbodiimide hydrochloride (EDC) (Chemical Dojin Co., Ltd., Osaka, Japan), N-hydroxysuccinimide (NHS), 99.5% ethanol and bovine serum albumin (BSA, FUJIFILM Wako Pure Chemical Corporation, Osaka, Japan) and PBS with 0.05% Tween 20, pH 7.4 (Sigma, St Louis, MO, USA).

A 30 MHz piezoelectric quartz wafer with twin gold electrodes, channel 1 (CH1) and channel 2 (CH2), is illustrated in Figure 1a. In our work, CH1 was used as an antibody-immobilized sensor, while CH2 was used as a reference sensor without antibody-immobilization. The measurement system shown in Figure 1b included a NAPiCOS system (Nihon Dempa Kogyo, Tokyo, Japan), a syringe pump (Harvard Apparatus, MA, USA) and a 6-port rotary injector (Rheodyne, CA, USA).

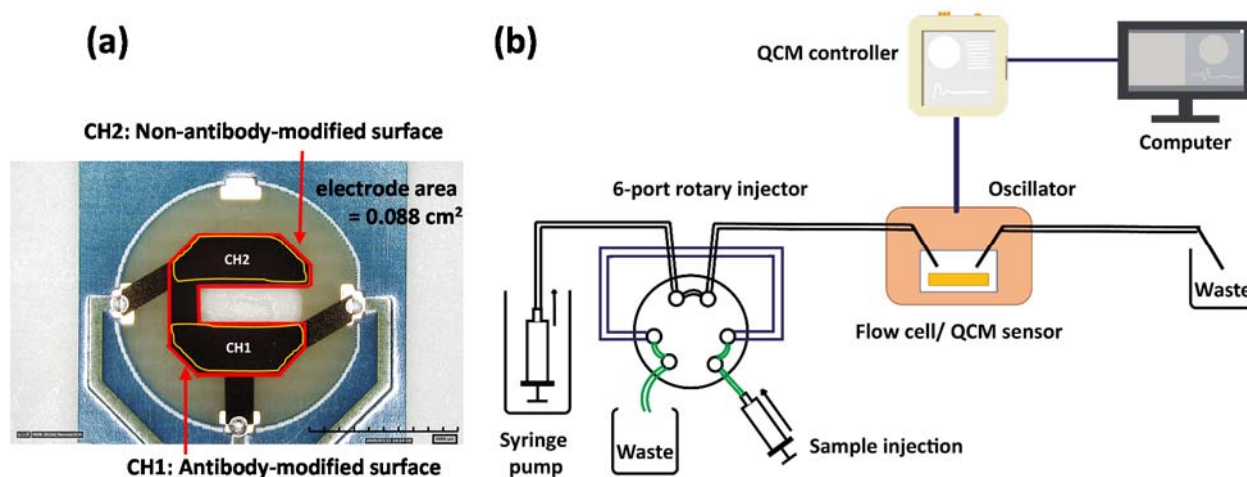


**Figure 1.** Measurement system: (a) QCM sensor chip surfaces; (b) schematic of the QCM sensing system for quantitative assessment of periodontal bacteria.

## 2.2. Self-Assembled Monolayer and Surface Characterization

The 11-mercaptoundecanoic acid (11-MUA) was used in this study. First, the gold surface was cleaned with 1 M sodium hydroxide and 1 M hydrochloric acid before surface modification [19]. Then, the surface of the gold electrode was modified with the 11-MUA.

For the formation of a self-assembled monolayer (SAM) of 11-MUA, 180  $\mu\text{L}$  of 2 mM 11-MUA in ethanol was applied to the gold surface and incubated for 12 h to form the SAM. After incubation, the gold surface was washed with ethanol and deionized water and dried with nitrogen gas. The evaluation for 11-MUA SAM on the gold surface was performed with the cyclic voltammetry technique using an Autolab PGSTAT100 and GPES software [20]. Briefly, the 11-MUA SAM-modified gold electrode was used as a working electrode. A platinum wire (diameter = 1 mm) and a silver (Ag)/silver chloride (AgCl) wire in a 3.3 M KCl solution with a salt bridge were used as the counter and the reference electrode, respectively. Ramp voltages were applied from  $-0.0$  to  $-1.2$  V with a scan rate of  $0.1$  V/s in a  $0.5$  M potassium hydroxide solution. The dissolved oxygen was removed from the solution by bubbling nitrogen gas before measurement. The total surface area of the gold electrode was  $0.176\text{ cm}^2$ . The SAM density was calculated with the peak area of the reduction current ( $Q_{\text{SAM}}$ ) from  $-0.80$  to  $-1.00$  V vs. Ag/AgCl at the first sweep. The density of the SAM on the gold surface was estimated using the following equation:

$$Y_{\text{SAM}} = Q_{\text{SAM}} N_{\text{A}} / FA \quad (1)$$

where  $N_A$ ,  $F$  and  $A$  are the Avogadro constant ( $6.02 \times 10^{23} \text{ mol}^{-1}$ ), Faraday constant ( $96,500 \text{ C mol}^{-1}$ ) and surface area ( $2 \times 8.8 \times 10^{12} \text{ nm}^2$ ), respectively.

### 2.3. Antibody Immobilization on a Carboxy-Terminated Self-Assembled Monolayer Surface

The antibody immobilization scheme on a carboxy-terminated SAM is shown in Figure 2.

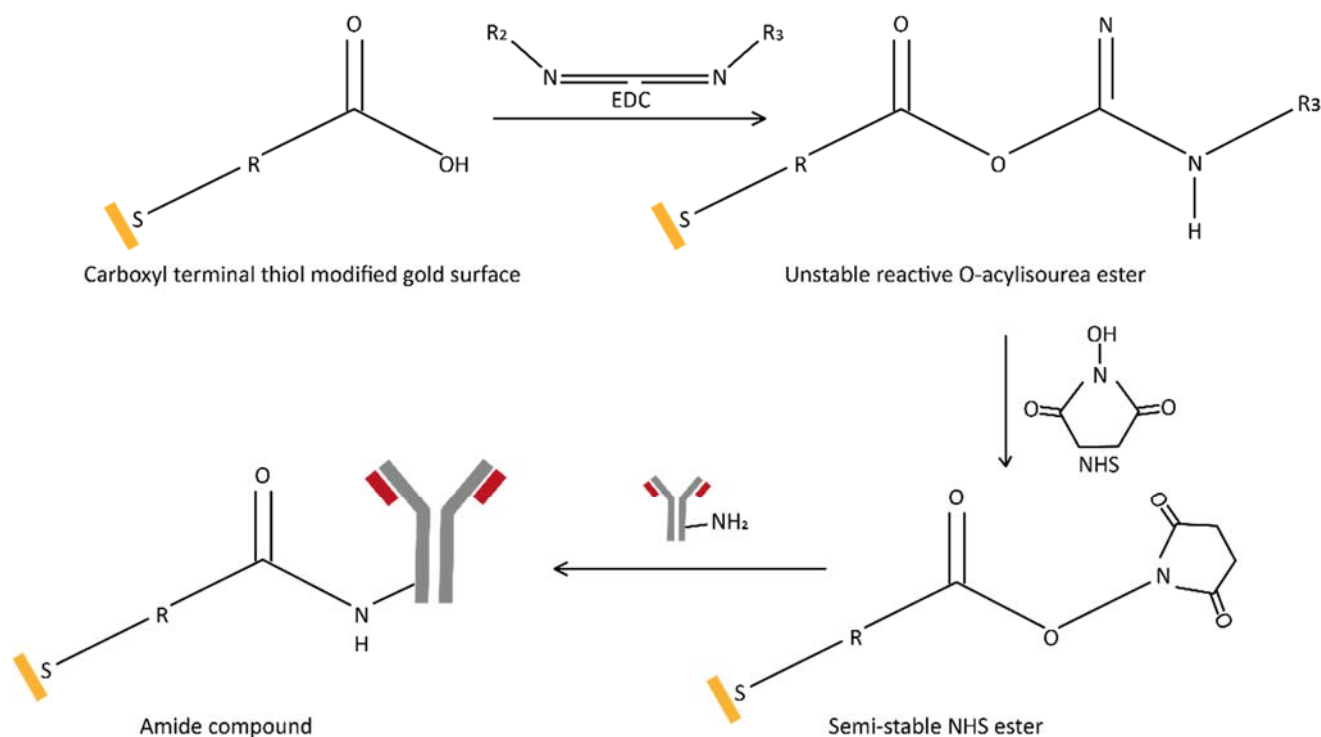


**Figure 2.** Strategy for immobilizing antibody to carboxylate-terminated SAM (11-MUA) on gold through EDC/NHS chemistry.

The 11-MUA modified surface was first activated by adding a mixed solution of 0.5 M NHS and 0.2 M EDC in deionized water and incubated for 90 min at room temperature. Then, 100  $\mu\text{L}$  of 5  $\mu\text{g/mL}$  anti-*A. actinomycetemcomitans* in 0.1 M acetate buffer (pH 5.0) were added directly to the activated SAM surface, while 0.1 M acetate buffer without antibody was used as negative control and incubated for 60 min at room temperature. The resulting immobilized surface was then washed with PBS, followed by 100  $\mu\text{L}$  of 1 M ethanolamine (pH 8.8) for 20 min to inactivate the unreacted esters of the gold surfaces. The frequency signals of the modified sensor in response to two types of bacteria were measured and compared in a real time.

### 2.4. Enzyme-Linked Immunosorbent Assay

An enzyme-linked immunosorbent assay (ELISA) was used to confirm the specific binding of anti-*A. actinomycetemcomitans* antibody used in this study. Standard 96-well microplates (Sumitomo Bakelite Co., Ltd., Osaka, Japan) and a microplate reader (Tecan Group Ltd., Männedorf, Switzerland) were used throughout the assays. Briefly, the wells of a microplate were individually seeded with  $1 \times 10^6$  cells/mL of *A. actinomycetemcomitans* and *P. gingivalis* and incubated at 37 °C overnight. BSA (2% (w/v)) was used as a blocking agent. Next, anti-*A. actinomycetemcomitans* antibody was then applied to *A. actinomycetemcomitans* and *P. gingivalis* coated wells and incubated for 30 min. After incubation, the coated wells were washed with 0.05% Tween 20 in PBS. Protein G-conjugated horseradish peroxidase (0.1  $\mu\text{g/mL}$ , Invitrogen™, Waltham, MA, USA), a secondary detector, was applied to the well and incubated for another hour at 25 °C. Unbound molecules were removed with PBS containing 0.1% (w/w) Tween 20. Finally, 3,3',5,5'-tetramethylbenzidine

(Abcam, Cambridge, UK) was added to the wells to generate the colorimetric reaction and 0.5 M sulfuric acid was used to stop the reaction. Optical density measurements were performed using a microplate reader at a wavelength of 450 nm.

### 2.5. Fabrication of the QCM Immunosensor

To fabricate the QCM immunosensor, the 11-MUA modification was performed on the gold surfaces (both CH1 and CH2) for 12 h at room temperature. The 11-MUA layer was activated by adding a mixed solution of 0.5 M NHS and 0.2 M EDC in deionized water (both CH1 and CH2) and incubated for 90 min at room temperature. Then, 100  $\mu$ L of 5  $\mu$ g/mL anti-*A. actinomycetemcomitans* antibody in 0.1 M acetate buffer (pH 5.0) were added directly to the activated CH1, while 0.1 M acetate buffer without antibody (negative control) was added to the activated CH2 and incubated for 60 min at room temperature. The resulting QCM sensors were then washed with PBS followed by 100  $\mu$ L of 1 M ethanolamine (pH 8.8) for 20 min to inactivate the unreacted esters of the Au surfaces.

### 2.6. Quartz Crystal Microbalance Measurement

For the detection of *A. actinomycetemcomitans*, the modified QCM chip was first equilibrated with PBS buffer for at least 10 min. Then, 200  $\mu$ L of *A. actinomycetemcomitans* samples at a concentration ranging from  $1.16 \times 10^3$  to  $1.16 \times 10^7$  cells/mL (10-fold serial dilution) were separately applied to the QCM measurement system via the 6-port rotary injector. The flow of the liquid phase was driven by the syringe pump with a flow rate of 50  $\mu$ L/min and PBS was used as a running buffer. The decrease in frequency caused by the binding of various concentrations of *A. actinomycetemcomitans* were measured in real time. The detection time was 1200 s. The background signal (obtained from CH2) was subtracted from the binding signal (obtained from CH1) and, thus, a real binding signal of each detection was used to obtain the calibration curve and the limit of detection was determined. The limit of detection was calculated based on the regression equation using the standard deviation of the blank samples with the confidence value of 3. Microscope imaging was also performed to confirm the binding of the target bacteria to the QCM electrode with immobilized antibody.

## 3. Results and Discussion

### 3.1. Characterization of the Self-Assembled Monolayer of 11-MUA

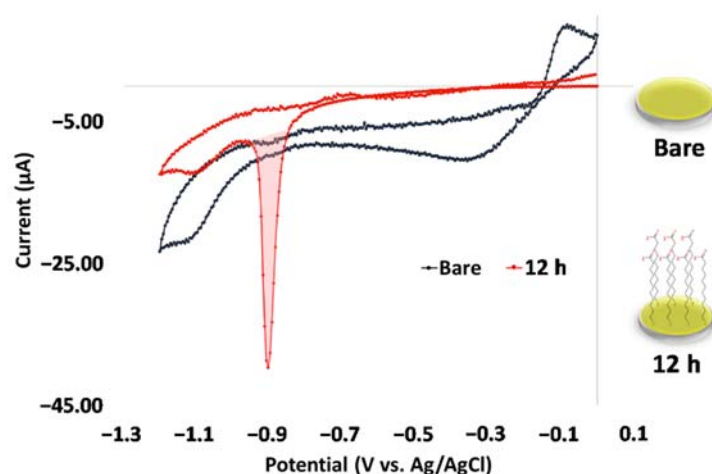
According to the results of the cyclic voltammetry measurement, as shown in Figure 3, the SAM density was confirmed as 4.46–4.54 molecules/nm<sup>2</sup>, which was a maximum density of alkanethiol molecules that could be adsorbed on the gold surface [21,22].

Table 1 shows the 11-MUA formation on the gold surface in both incubation times of 12 h and 24 h. The amount of 11-MUA on the gold area of the QCM sensor can be 144 ng/cm<sup>2</sup> for both incubation times. The surface modification time of 12 h had better repeatability and was used in the next study.

**Table 1.** Mass changes of the 11-MUA-modified QCM sensor chips converted from frequency changes at 12 and 24 h of incubation.

Incubation Time (h)	AUC ( $Q_{SAM}$ , C)	Packing Density (Molecule·nm <sup>−2</sup> )	Weight <sub>11-MUA</sub> on Au Surface (ng)
12	$1.28 \times 10^{-5}$ ( <i>n</i> = 4)	4.54	144.5
24	$1.26 \times 10^{-5}$ ( <i>n</i> = 2)	4.46	142.3





**Figure 3.** Characterization of the self-assembled monolayer of 11-MUA on a gold electrode by cyclic voltammetry. The cyclic voltammograms of the bare gold electrode (black) and 11-MUA-modified gold electrode (red) after 12 h of 11-MUA modification. The cyclic voltammogram of 11-MUA-modified-gold indicates the Au-S bond reduction peak area at  $-0.95$  V vs. Ag/AgCl (red area). Electrodes: working electrode, Au; counter electrode, Pt; reference electrode, Ag/AgCl wire (in 3.3 M KCl with a salt bridge). Scan rate: 0.1 V/s.

### 3.2. Specificity of Anti-*A. actinomycetemcomitans* Antibody

The ELISA experiment was performed to check the specificity of the antibody used in this study. *A. actinomycetemcomitans* and *P. gingivalis* cells were separately seeded in a 96-well plate overnight. Then, anti-*A. actinomycetemcomitans* antibody was added to test the binding with two different types of bacteria. The results shown in Figure 4 revealed that the absorbance at the wavelength of 450 nm was observed only in *A. actinomycetemcomitans* coated wells. The color of the *A. actinomycetemcomitans* coated wells turned yellow, while color change was not observed in *P. gingivalis* coated wells, as can be seen in Figure 4a. The concentration-dependent absorption at 450 nm could be obtained only for *A. actinomycetemcomitans* coated wells, as shown in Figure 4b. Thus, the specificity of the antibody for the detection of *A. actinomycetemcomitans* could be proved in the ELISA experiments.

### 3.3. Determination of the Bacteria Concentration and Calibration Curves

QCM measurements were performed to determine the concentration of bacteria that were bound to their specific antibody on the modified gold surface of the QCM chip. As described previously, anti-*A. actinomycetemcomitans* antibody was immobilized on the gold surface using the 11-MUA SAM.

Figure 5b shows comparison of the responses of the QCM sensor to *A. actinomycetemcomitans*, *P. gingivalis*, *P. nigrescens* and *A. naeslundii*, respectively. The frequency signal of the QCM sensor gradually decreased upon adding the *A. actinomycetemcomitans* cells (200  $\mu$ L of  $1.16 \times 10^8$  cells/mL) to the QCM surface and the frequency shift reached about 120 Hz in 7 min. On the other hand, the frequency shift could not be observed when *P. gingivalis* cells (200  $\mu$ L of  $1.16 \times 10^8$  cells/mL), *P. nigrescens* cells (200  $\mu$ L of  $1.16 \times 10^8$  cells/mL) and *A. naeslundii* cells (200  $\mu$ L of  $1.16 \times 10^8$  cells/mL) were added to the sensor surface. Excellent specificity was therefore confirmed for detection of *A. actinomycetemcomitans* using the functionalized QCM chip with the 11-MUA SAM. The study by Reeves et al., 2014, confirmed the usability of *A. actinomycetemcomitans* mAb (325AA2) [23]. The monoclonal antibody was shown to be highly specific for *A. actinomycetemcomitans* cells [24].

For the calibration curve, 10-fold diluted solutions of *A. actinomycetemcomitans* cells were separately injected into the flow system. The response profiles of the QCM sensors to various concentrations of bacteria are shown in Figure S1 in the Supplementary Materials. Figure 6a shows the typical examples of the time courses for the frequency changes of the functionalized QCM chip in response to various concentrations of *A. actinomycetemcomitans*.

The frequencies decreased in a concentration-dependent manner. The frequency shifts were approximately 7, 16, 24, 40 and 67 Hz for the numbers of *A. actinomycetemcomitans* cells in the range from 232 to  $2.32 \times 10^6$  cells. Figure 6b shows the calibration curve for *A. actinomycetemcomitans*, illustrating the correlation between the frequency shifts and the number of bacteria. Based on a regression equation, the lower detection limit was 800 cells with a dynamic range up to  $2.32 \times 10^6$  cells. Figure 6c shows the photographs of the surface of the functionalized QCM chip before and after adding the *A. actinomycetemcomitans* cells at the concentration of  $1.16 \times 10^8$  cells/mL. The surface functionalized with anti-*A. actinomycetemcomitans* antibody using the 11-MUA SAM was found to capture *A. actinomycetemcomitans* cells directly, suggesting that the antibody immobilization was successful and that bacteria attachment was rigid. These results clearly indicated that the frequency responses were resulted from specific binding after *A. actinomycetemcomitans* injection.

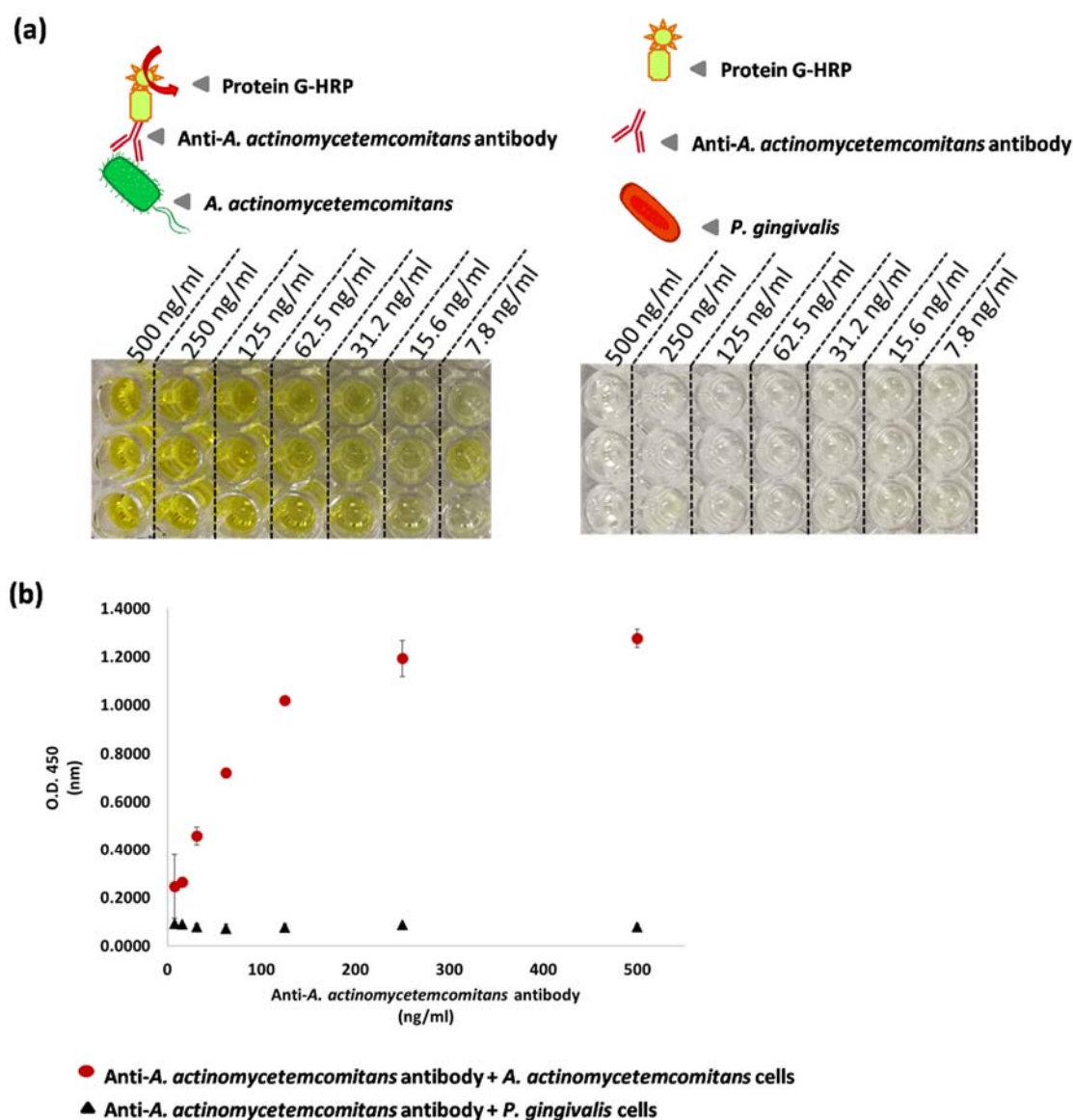


**Figure 4.** Specificity of Anti-*A. actinomycetemcomitans* antibody. Anti-*A. actinomycetemcomitans* antibody specifically binds to *A. actinomycetemcomitans* cells and not to *P. gingivalis* cells. (a) A 96-well plate of Anti-*A. actinomycetemcomitans* antibody and *A. actinomycetemcomitans* cells (left). A 96-well plate of Anti-*A. actinomycetemcomitans* antibody and *P. gingivalis* cells (right). (b) ELISA results when executed with different concentrations of Anti-*A. actinomycetemcomitans* antibody for *A. actinomycetemcomitans* (red). *P. gingivalis* cells (black) were used as negative control. Mean and SD values were obtained from three measurements.

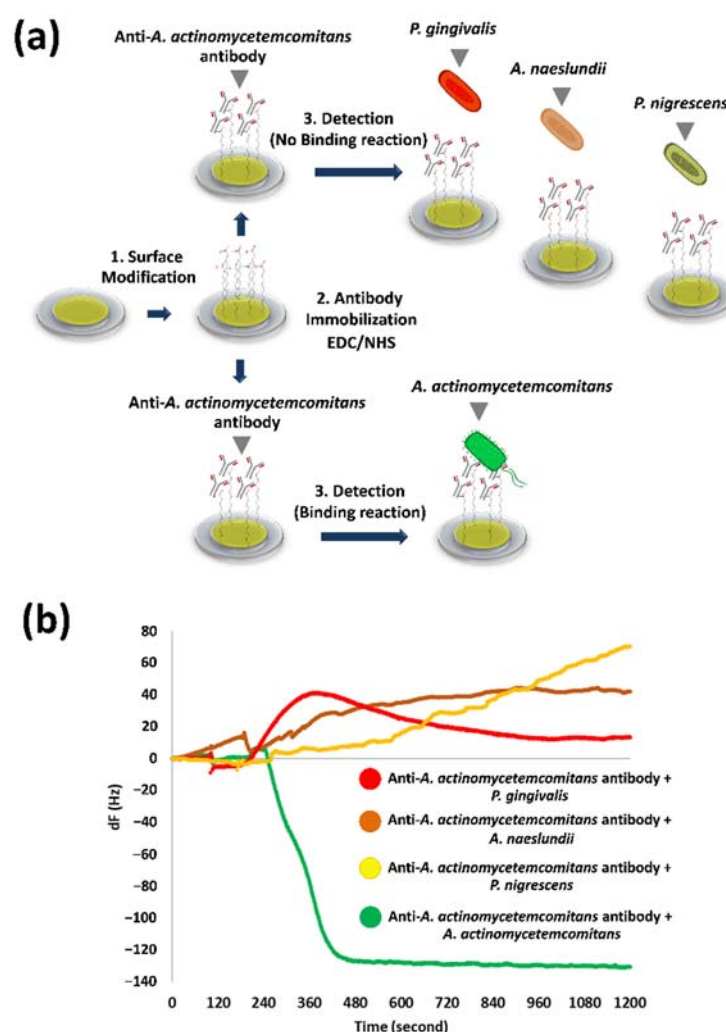


**Figure 5.** Selectivity of the modified QCM sensor. (a) The processes of the 11-MUA formation on a gold electrode in conjunction with immobilization of antibodies and binding reaction are schematically shown. (b) The representative response profile of *A. actinomycetemcomitans* antibody-immobilized sensors for *A. actinomycetemcomitans* (green line) detection is shown, while *P. gingivalis* (red line), *P. nigrescens* (yellow line) and *A. naeslundii* (brown line) were used as negative control.

The limit of detection for the functionalized QCM chip developed in this study is comparable with other detection platforms, such as impedance detection, potentiometry, or surface plasmon resonance. Conventional detection methods of periodontal bacteria suffer from the multistep processing, such as bacteria culture and labelling of several reagents and signal enhancers. Among several kinds of periodontal bacteria, the threshold concentrations for *T. denticola* and *P. intermedia* were reported to be more than 100 folds higher than the threshold for *A. actinomycetemcomitans* [10], suggesting that the latter species may be more virulent. The relatively low threshold concentration for *A. actinomycetemcomitans* was also reported in other studies [25,26]. Their findings suggested that the levels above the critical threshold concentration would serve as a better predictor of periodontitis than its presence or absence. In our study, the specific antibody was used to develop the QCM immunosensor for the detection of *A. actinomycetemcomitans*, a periodontal pathogen and quantitative detection with a dynamic range up to  $2.32 \times 10^6$  cells. Moreover, a response time of 20 min has been demonstrated without any labelling materials.



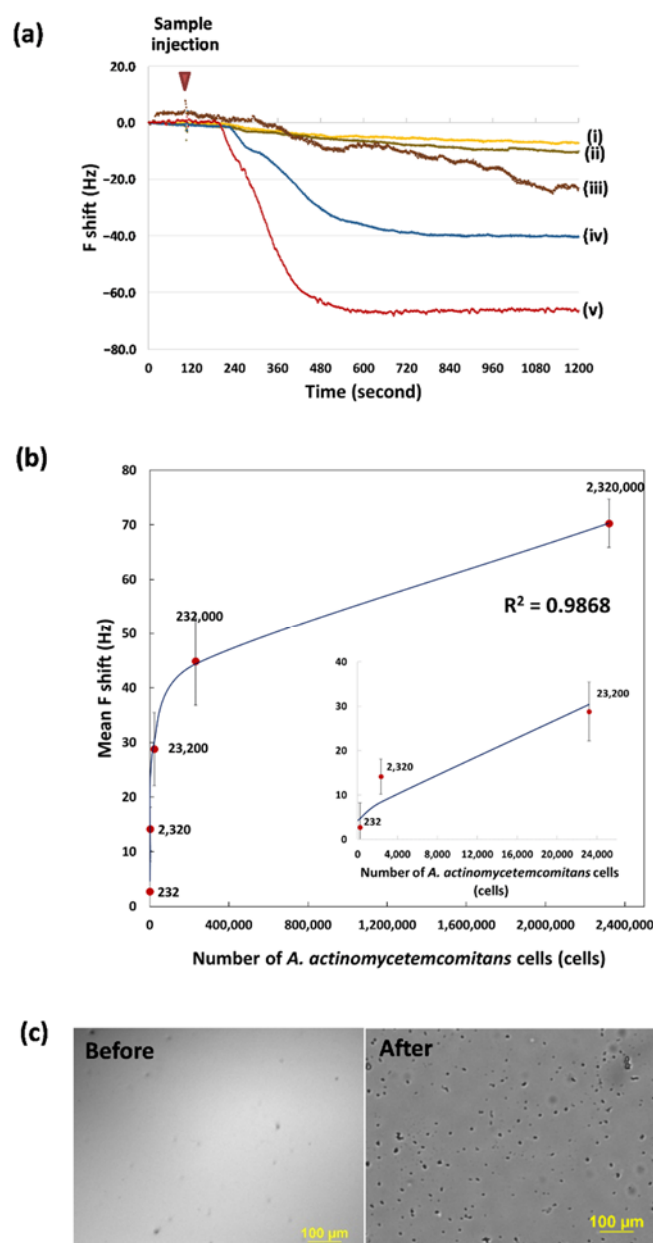


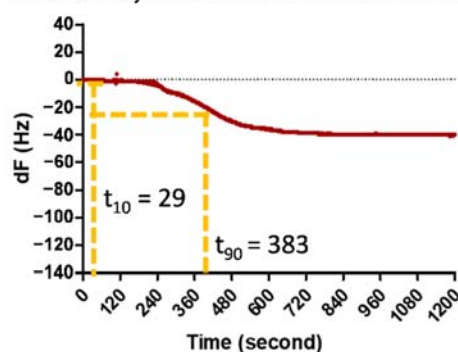
**Figure 6.** Label-free periodontal bacteria detection using QCM measurements. **(a)** The representative sensorgram showing the sensor response at different *A. actinomycetemcomitans* concentrations: 200  $\mu\text{L}$  *A. actinomycetemcomitans* suspension having: (i)  $1.16 \times 10^3$ ; (ii)  $1.16 \times 10^4$ ; (iii)  $1.16 \times 10^5$ ; (iv)  $1.16 \times 10^6$  and (v)  $1.16 \times 10^7$  cells/mL. **(b)** The calibration curve of the QCM immunoassay for *A. actinomycetemcomitans* illustrating the correlation between frequency shift and bacterial number. The mean and SD values were obtained from three measurements. **(c)** Optical microscopy visualization of the QCM sensor surface. The images are obtained from the bare gold surface (before surface modification) and after injection of *A. actinomycetemcomitans* ( $1.16 \times 10^8$  cells/mL) on the modified QCM sensor.

### 3.4. Response Time Analysis for the Frequency Shift

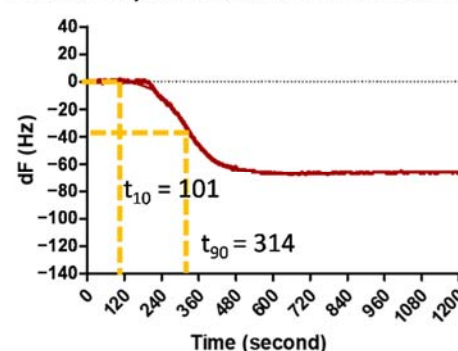
The frequency shifts (1200 datapoints) from all binding conditions were also used for analyzing the response times to investigate the binding kinetics between the antibody and the cell. In Figure 7, the curve fitting was performed by using nonlinear regression analysis. The times which are required for the QCM signal to reach 10% and 90% of the saturated values are expressed as  $t_{10}$  and  $t_{90}$ , respectively. The  $t_{10}$  and  $t_{90}$  were calculated from the equation of the fitted curve and the response time ( $\tau$ ) of the binding was defined as the

difference between  $t_{90}$  and  $t_{10}$ . The response times were compared among each *A. actinomycetemcomitans* concentration, as shown in Table 2. It was found that the mean of the  $\tau$  values decreased from 243 to 134 s, when the concentration of the *A. actinomycetemcomitans* cells increased from  $1.16 \times 10^6$  to  $1.16 \times 10^8$ .

*A. actinomycetemcomitans*  $1.16 \times 10^6$  cells/ml



*A. actinomycetemcomitans*  $1.16 \times 10^7$  cells/ml



*A. actinomycetemcomitans*  $1.16 \times 10^8$  cells/ml

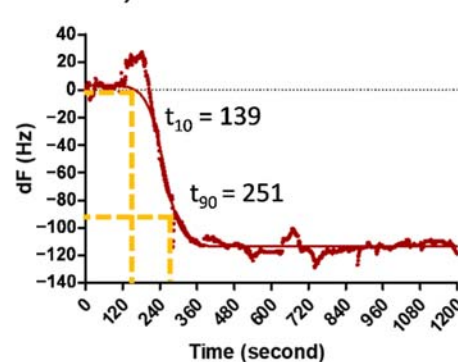


**Figure 7.** The  $t_{10}$  and  $t_{90}$  obtained from the fitted curve of the measurements are indicated by the yellow lines.

**Table 2.** Response time of the binding between *A. actinomycetemcomitans* cells and Anti-*A. actinomycetemcomitans* antibody.

<i>A. actinomycetemcomitans</i> Cells Density (Cells/mL)		$t_{10}$	$t_{90}$	Response Time ( $\tau = t_{90} - t_{10}$ )
$1.16 \times 10^6$	N1	124	302	177
	N2	29	383	354
	N3	185	384	198
	mean	113	356	243
	SD	64.2	38.5	78.6
$1.16 \times 10^7$	N1	230	274	44
	N2	101	314	212
	N3	24	409	385
	mean	119	332	214
	SD	84.7	56.7	138.9
$1.16 \times 10^8$	N1	139	251	112
	N2	137	289	152
	N3	201	339	138
	mean	159	293	134
	SD	29.6	36.0	16.5

The mean and SD values were obtained from three measurements.

In the measurement system and the protocol in this study, *A. actinomycetemcomitans* cells in a sample solution were captured on the antibody modified QCM surface during the continuous sample flow. The binding between the immobilized antibody and the bacterial surface antigen was therefore performed at non-equilibrium state. In such a case, transient cell–surface interactions occur in addition to adhesion and binding at the surface of the antibody modified QCM. Some cells, such as MCF-7 cells and mesenchymal stem cells, were reported to exhibit the rolling behavior on specific antibody-immobilized surfaces under continuous flow conditions [27,28]. Cell rolling involves continuous formation and dissociation of affinity bonds between cells and the surface under fluid flow. On the surface of the gold electrode of the QCM sensor, the antibody was immobilized with high density and *A. actinomycetemcomitans* cells could be captured on the QCM surface with multi-site binding after transient cell–surface molecular interactions. Multi-site binding was effective to enhance binding strength and capturing efficiency [22,29]. As shown in Figure 7 and Table 2, the response time of the QCM sensor became shorter when the concentration of *A. actinomycetemcomitans* cells increased from  $1.16 \times 10^6$  to  $1.16 \times 10^8$  cells/mL, because the collision probability of the cells to the surface increased in the higher concentration. Cell capture performance was reported to be improved by increasing cell–substrate contact frequency using three-dimensional twisting flow with a patterned nanostructured channel. [30] Control of orientation of the immobilized antibody on the gold electrode would also be important to improve capture performance of the bacterial cells. The detailed study of the binding kinetic between antibody and the cell under flow condition is now in the process.

A comparison of the different detection methods for bacterial cells is given in Table 3. Although potentiometric and amperometric detection methods show better sensitivity, pretreatment of bacteria or secondary enzymatic reaction are required. The limit of detection achieved in this study was more or less similar to those of the reported methods using QCM and surface plasmon resonance (SPR) technique. Although, SPR and QCM have many features in common, they measure the signal in different ways. SPR detects the change in permittivity based on the plasmonic principle and is less sensitive to mechanical disruptions and viscoelastic effects. QCM measures the frequency of oscillations for a thin film deposited on the surface [31]. The method and the device developed in this study would be useful for assessment of periodontal disease.

**Table 3.** Performance of the different biosensor types for bacterial detection.

Target Pathogen	Transducer	Sensing Strategy	Limit of Detection	Ref.
<i>P. gingivalis</i> <i>E. coli</i>	Microfluidic cell-hydrodynamic focusing	No immobilization, impedance reading during sample flow	$10^3$ cells/mL	[32]
Sulfate-reducing bacteria	Glassy carbon electrode	Potentiometric analysis, bacterial processing is required	$2.3 \times 10^{-2.3} \times 10^7$ CFU/mL	[33]
Heat-killed <i>E. coli</i>	Saturated calomel electrode	Amperometric detection of secondary antibody using glucose oxidase	$3 \times 10^1 - 3.2 \times 10^6$ CFU/mL	[34]
<i>S. oneidensis</i>	SERS	Silver nanoparticles sandwiched by analyte binding on optical fiber tip	$10^6$ cells/mL	[35]
<i>E. coli</i> <i>S. aureus</i> <i>B. subtilis</i>	SPR	Lectin-functionalized anisotropic silver nanoparticles	$1.5 \times 10^4$ CFU/mL	[36]
<i>E. coli</i> O157:H7	QCM	Antibody for capture, antibody-functionalized nanoparticles for signal enhancement	$10^6$ cells/mL	[37]
<i>A. actinomycetemcomitans</i>	QCM	Antibody immobilization by using 11-MUA-EDC/NHS	$1.16 \times 10^4$ cells/mL	This study

Abbreviations: SERS, surface-enhanced Raman scattering; SPR, surface plasmon resonance; QCM, quartz crystal microbalance; CFU, colony-forming unit.

Overall, QCM measurement, in this study, is an effective method that enables extremely sensitive, quantitative, real-time, label-free and noninvasive detection of molecules adsorbed on a solid surface.

#### 4. Conclusions

We have successfully developed a cell-based immunoassay for the detection of *A. actinomycetemcomitans* utilizing a QCM sensor. A specific antibody was immobilized on the surface of the QCM chip and therefore the developed method did not require a labelling process. Simple, rapid and sensitive detection of periodontal bacteria would be realized just by adding the sample solution containing bacteria onto the surface of the QCM chip. In the present study, dual gold electrodes formed on the surface of the quartz substrate were used as a sample and a reference QCM sensor, respectively. It is possible to integrate several gold electrodes on the single quartz substrate for simultaneous detection of multiple periodontal bacteria. In order to understand periodontal disease in more detail and predict progression of periodontitis, it is desirable to analyze information of multiple bacteria simultaneously. Periodontal disease is a complex host response composed of a broad array of inflammatory cells and the mediators derived from cells resident in the gingival tissues, as well as emigrating inflammatory cells. Recent studies revealed that Gram-negative anaerobic bacteria, such as *A. actinomycetemcomitans*, *P. gingivalis*, *T. forsythia*, *T. denticola* and *P. intermedia*, were strongly associated with periodontal disease [10,38]. Moreover, the development of periodontal and peri-implant lesions was reported to be related to real raise of bacterial counts estimated for *A. actinomycetemcomitans*, *P. gingivalis*, *T. forsythia*, *P. intermedia*, *T. denticola* [39]. Based on the method and the device developed in this study, integrated QCM sensors with different kinds of antibodies can be developed to detect the above five bacteria simultaneously and to analyze the trends of the concentrations of these bacteria for clinical diagnostics of periodontal disease at an early stage. Since the QCM technology is well established and reliable measurements can be performed with a small instrument, our device would be useful as a simple, rapid and sensitive detection tool not only for clinical research but also for a chairside device in a dental office.

**Supplementary Materials:** The following are available online at <https://www.mdpi.com/article/10.3390/chemosensors9070159/s1>, Figure S1: Response profiles of *A. actinomycetemcomitans* antibody-immobilized sensors for *A. actinomycetemcomitans* cells detection.

**Author Contributions:** Conceptualization, Y.M., M.T. and S.R.; methodology, S.R.; C.R. and W.B.; software, S.R. and P.S.; validation, S.R. and M.S.; formal analysis, S.R. and M.S.; investigation, Y.M. and M.S.; resources, Y.M., M.T. and Y.T.; data curation, S.R.; writing—original draft preparation, S.R.; writing—review and editing, S.R., Y.M., M.S. and M.T.; visualization, S.R.; supervision, Y.M., M.S. and M.T.; project administration, M.T.; funding acquisition, S.R., Y.M., M.S. and M.T. All authors have read and agreed to the published version of the manuscript.

**Funding:** This work was supported in part by the OVERSEAS RESEARCH EXPERIENCE SCHOLARSHIP for Graduate Student, Graduate School and Faculty of Engineering, Chulalongkorn University, by THE JAPAN SCIENCE AND TECHNOLOGY AGENCY (JST) through COI Grant Number JPMJCE1305, by THE MINISTRY OF EDUCATION, CULTURE, SPORTS, SCIENCE AND TECHNOLOGY (MEXT) as part of the Research Center for Biomedical Engineering and by THE NIPPON SHEET GLASS FOUNDATION FOR MATERIALS SCIENCE AND ENGINEERING.

**Conflicts of Interest:** The authors declare that they have no known competing financial interests or personal relationships that could have appeared to influence the work reported in this paper.

## References

1. Chang, H.-J.; Lee, S.-J.; Yong, T.-H.; Shin, N.-Y.; Jang, B.-G.; Kim, J.-E.; Huh, K.-H.; Lee, S.-S.; Heo, M.-S.; Choi, S.-C.; et al. Deep Learning Hybrid Method to Automatically Diagnose Periodontal Bone Loss and Stage Periodontitis. *Sci. Rep.* **2020**, *10*, 7531. [\[CrossRef\]](#)
2. He, W.; You, M.; Wan, W.; Xu, F.; Li, F.; Li, A. Point-of-Care Periodontitis Testing: Biomarkers, Current Technologies, and Perspectives. *Trends Biotechnol.* **2018**, *36*, 1127–1144. [\[CrossRef\]](#)
3. Dewhirst, F.E.; Chen, T.; Izard, J.; Paster, B.J.; Tanner, A.C.R.; Yu, W.-H.; Lakshmanan, A.; Wade, W.G. The Human Oral Microbiome. *J. Bacteriol.* **2010**, *192*, 5002. [\[CrossRef\]](#)
4. Hajishengallis, G.; Liang, S.; Payne, M.A.; Hashim, A.; Jotwani, R.; Eskin, M.A.; McIntosh, M.L.; Alsam, A.; Kirkwood, K.L.; Lambris, J.D.; et al. Low-Abundance Biofilm Species Orchestrates Inflammatory Periodontal Disease through the Commensal Microbiota and Complement. *Cell Host Microbe* **2011**, *10*, 497–506. [\[CrossRef\]](#) [\[PubMed\]](#)
5. Slots, J. Periodontitis: Facts, fallacies and the future. *Periodontology 2000* **2017**, *75*, 7–23. [\[CrossRef\]](#)
6. Nomura, Y.; Takeuchi, H.; Okamoto, M.; Sogabe, K.; Okada, A.; Hanada, N. Chair-side detection of *Prevotella Intermedia* in mature dental plaque by its fluorescence. *Photodiagn. Photodyn. Ther.* **2017**, *18*, 335–341. [\[CrossRef\]](#) [\[PubMed\]](#)
7. Suzuki, N.; Yoneda, M.; Hirofujii, T. Mixed Red-Complex Bacterial Infection in Periodontitis. *Int. J. Dent.* **2013**, *2013*, 587279. [\[CrossRef\]](#)
8. Park, O.J.; Yi, H.; Jeon, J.H.; Kang, S.S.; Koo, K.T.; Kum, K.Y.; Chun, J.; Yun, C.H.; Han, S.H. Pyrosequencing Analysis of Subgingival Microbiota in Distinct Periodontal Conditions. *J. Dent. Res.* **2015**, *94*, 921–927. [\[CrossRef\]](#) [\[PubMed\]](#)
9. Scapoli, L.; Girardi, A.; Palmieri, A.; Martinelli, M.; Cura, F.; Lauritano, D.; Carinci, F. Quantitative Analysis of Periodontal Pathogens in Periodontitis and Gingivitis. *J. Biol. Regul. Homeost. Agents* **2015**, *29*, 101–110. [\[PubMed\]](#)
10. Torrungruang, K.; Jitpakdeebordin, S.; Charatkulangkun, O.; Gleebua, Y. *Porphyromonas gingivalis*, *Aggregatibacter actinomycetemcomitans*, and *Treponema denticola*/*Prevotella intermedia* Co-Infection are Associated with Severe Periodontitis in a Thai Population. *PLoS ONE* **2015**, *10*, e0136646. [\[CrossRef\]](#)
11. Ahmed, A.; Rushworth, J.V.; Hirst, N.A.; Millner, P.A. Biosensors for Whole-Cell Bacterial Detection. *Clin. Microbiol. Rev.* **2014**, *27*, 631. [\[CrossRef\]](#) [\[PubMed\]](#)
12. Malagi, S. Chairside Diagnostic Test Kits In Periodontics—A Review. *Int. Arab J. Dent.* **2015**, *30*, 99–102.
13. Ravishankar, P.; Mithra, D.; Chakraborty, P.; Kumar, A. Chairside diagnostics in periodontics. *SRM J. Res. Dent. Sci.* **2017**, *8*, 78–81. [\[CrossRef\]](#)
14. Yamamoto, Y. PCR in diagnosis of infection: Detection of bacteria in cerebrospinal fluids. *Clin. Diagn. Lab. Immunol.* **2002**, *9*, 508–514. [\[CrossRef\]](#)
15. Brosel-Oliu, S.; Abramova, N.; Uria, N.; Bratov, A. Impedimetric transducers based on interdigitated electrode arrays for bacterial detection—A review. *Anal. Chim. Acta* **2019**, *1088*, 1–19. [\[CrossRef\]](#) [\[PubMed\]](#)
16. Chen, J.Y.; Penn, L.S.; Xi, J. Quartz crystal microbalance: Sensing cell-substrate adhesion and beyond. *Biosens. Bioelectron.* **2018**, *99*, 593–602. [\[CrossRef\]](#) [\[PubMed\]](#)
17. Uekubo, A.; Hiratsuka, K.; Aoki, A.; Takeuchi, Y.; Abiko, Y.; Izumi, Y. Effect of antimicrobial photodynamic therapy using rose bengal and blue light-emitting diode on *Porphyromonas gingivalis* in vitro: Influence of oxygen during treatment. *Laser Ther.* **2016**, *25*, 299–308. [\[CrossRef\]](#) [\[PubMed\]](#)
18. Komazaki, R.; Katagiri, S.; Takahashi, H.; Maekawa, S.; Shiba, T.; Takeuchi, Y.; Kitajima, Y.; Ohtsu, A.; Udagawa, S.; Sasaki, N.; et al. Periodontal pathogenic bacteria, *Aggregatibacter actinomycetemcomitans* affect non-alcoholic fatty liver disease by altering gut microbiota and glucose metabolism. *Sci. Rep.* **2017**, *7*, 13950. [\[CrossRef\]](#)
19. Hai, W.; Goda, T.; Takeuchi, H.; Yamaoka, S.; Horiguchi, Y.; Matsumoto, A.; Miyahara, Y. Human influenza virus detection using sialyllactose-functionalized organic electrochemical transistors. *Sens. Actuators B Chem.* **2018**, *260*, 635–641. [\[CrossRef\]](#)



20. Goda, T.; Miyahara, Y. Thermo-responsive molecular switches for ATP using hairpin DNA aptamers. *Biosens. Bioelectron.* **2011**, *26*, 3949–3952. [[CrossRef](#)]
21. Poirier, G.E.; Tarlov, M.J.; Rushmeier, H.E. Two-Dimensional Liquid Phase and the px.sqroot.3 Phase of Alkanethiol Self-Assembled Monolayers on Au(111). *Langmuir* **1994**, *10*, 3383–3386. [[CrossRef](#)]
22. Horiguchi, Y.; Goda, T.; Matsumoto, A.; Takeuchi, H.; Yamaoka, S.; Miyahara, Y. Direct and label-free influenza virus detection based on multisite binding to sialic acid receptors. *Biosens. Bioelectron.* **2017**, *92*, 234–240. [[CrossRef](#)] [[PubMed](#)]
23. Reeves, B.D.; Young, M.; Grieco, P.A.; Suci, P. Aggregatibacter actinomycetemcomitans biofilm killing by a targeted ciprofloxacin prodrug. *Biofouling* **2013**, *29*, 1005–1014. [[CrossRef](#)]
24. Gmur, R. Monoclonal antibodies for the rapid identification in clinical samples of Peptostreptococcus micros and Actinobacillus actinomycetemcomitans serotypes a, d, and e. *Med. Microbiol. Lett.* **1996**, *5*, 335–349.
25. Papapanou, P.N.; Teanpaisan, R.; Obiechina, N.S.; Pithpornchaiyakul, W.; Pongpaisal, S.; Pisuthanakan, S.; Baelum, V.; Fejerskov, O.; Dahlén, G. Periodontal microbiota and clinical periodontal status in a rural sample in southern Thailand. *Eur. J. Oral Sci.* **2002**, *110*, 345–352. [[CrossRef](#)] [[PubMed](#)]
26. Laine, M.L.; Moustakis, V.; Koumakis, L.; Potamias, G.; Loos, B.G. Modeling Susceptibility to Periodontitis. *J. Dent. Res.* **2012**, *92*, 45–50. [[CrossRef](#)]
27. Mahara, A.; Yamaoka, T. Continuous separation of cells of high osteoblastic differentiation potential from mesenchymal stem cells on an antibody-immobilized column. *Biomaterials* **2010**, *31*, 4231–4237. [[CrossRef](#)]
28. Myung, J.H.; Launier, C.A.; Eddington, D.T.; Hong, S. Enhanced Tumor Cell Isolation by a Biomimetic Combination of E-selectin and anti-EpCAM: Implications for the Effective Separation of Circulating Tumor Cells (CTCs). *Langmuir* **2010**, *26*, 8589–8596. [[CrossRef](#)]
29. Myung, J.H.; Gajjar, K.A.; Chen, J.; Molokie, R.E.; Hong, S. Differential detection of tumor cells using a combination of cell rolling, multivalent binding, and multiple antibodies. *Anal. Chem.* **2014**, *86*, 6088–6094. [[CrossRef](#)]
30. Stroock, A.D.; Dertinger, S.K.; Ajdari, A.; Mezic, I.; Stone, H.A.; Whitesides, G.M. Chaotic mixer for microchannels. *Science* **2002**, *295*, 647–651. [[CrossRef](#)] [[PubMed](#)]
31. Fang, J.; Ren, C.; Zhu, T.; Wang, K.; Jiang, Z.; Ma, Y. Comparison of the different responses of surface plasmon resonance and quartz crystal microbalance techniques at solid–liquid interfaces under various experimental conditions. *Analyst* **2015**, *140*, 1323–1336. [[CrossRef](#)]
32. Zhu, T.; Pei, Z.; Huang, J.; Xiong, C.; Shi, S.; Fang, J. Detection of bacterial cells by impedance spectra via fluidic electrodes in a microfluidic device. *Lab Chip* **2010**, *10*, 1557–1560. [[CrossRef](#)]
33. Wan, Y.; Zhang, D.; Hou, B. Selective and specific detection of sulfate-reducing bacteria using potentiometric stripping analysis. *Talanta* **2010**, *82*, 1608–1611. [[CrossRef](#)]
34. Li, Y.; Fang, L.; Cheng, P.; Deng, J.; Jiang, L.; Huang, H.; Zheng, J. An electrochemical immunosensor for sensitive detection of Escherichia coli O157:H7 using C60 based biocompatible platform and enzyme functionalized Pt nanochains tracing tag. *Biosens. Bioelectron.* **2013**, *49*, 485–491. [[CrossRef](#)] [[PubMed](#)]
35. Yang, X.; Gu, C.; Qian, F.; Li, Y.; Zhang, J.Z. Highly Sensitive Detection of Proteins and Bacteria in Aqueous Solution Using Surface-Enhanced Raman Scattering and Optical Fibers. *Anal. Chem.* **2011**, *83*, 5888–5894. [[CrossRef](#)]
36. Gasparyan, V.K.; Bazukyan, I.L. Lectin sensitized anisotropic silver nanoparticles for detection of some bacteria. *Anal. Chim. Acta* **2013**, *766*, 83–87. [[CrossRef](#)]
37. Jiang, X.; Wang, R.; Wang, Y.; Su, X.; Ying, Y.; Wang, J.; Li, Y. Evaluation of different micro/nanobeads used as amplifiers in QCM immunosensor for more sensitive detection of E. coli O157:H7. *Biosens. Bioelectron.* **2011**, *29*, 23–28. [[CrossRef](#)] [[PubMed](#)]
38. Farias, B.C.; Souza, P.R.E.; Ferreira, B.; Melo, R.S.A.; Machado, F.B.; Gusmão, E.S.; Cimões, R. Occurrence of periodontal pathogens among patients with chronic periodontitis. *Braz. J. Microbiol.* **2012**, *43*, 909–916. [[CrossRef](#)] [[PubMed](#)]
39. Nastych, O.; Goncharuk-Khomyn, M.; Foros, A.; Cavalcanti, A.; Yavuz, I.; Tsaryk, V. Comparison of Bacterial Load Parameters in Subgingival Plaque during Peri-implantitis and Periodontitis Using the RT-PCR Method. *Acta Stomatol. Croat.* **2020**, *54*, 32–43. [[CrossRef](#)] [[PubMed](#)]